Heart wall velocimetry and exogenous contrast-based cardiac flow imaging in *Drosophila melanogaster* using Doppler optical coherence tomography

Michael A. Choma
Children's Hospital Boston
300 Longwood Avenue
Boston, Massachusetts 02115
and
Harvard Medical School
Department of Pediatrics
Boston, Massachusetts 02115

Melissa J. Suter
Massachusetts General Hospital
Wellman Center for Photomedicine
Boston, Massachusetts 02114
and
Harvard Medical School
Department of Dermatology
Boston, Massachusetts 02115

Benjamin J. Vakoc
Brett E. Bouma
Massachusetts General Hospital
Wellman Center for Photomedicine
Boston, Massachusetts 02114
and
Harvard Medical School
Department of Dermatology
Boston, Massachusetts 02115
and
Harvard-MIT Division of Health Sciences and Technology
77 Massachusetts Avenue
Cambridge, Massachusetts 02139

Guillermo J. Tearney
Massachusetts General Hospital
Wellman Center for Photomedicine
Boston, Massachusetts 02114
and
Harvard-MIT Division of Health Sciences and Technology
77 Massachusetts Avenue
Cambridge, Massachusetts 02139
and
Harvard Medical School
Department of Pathology
Boston, Massachusetts 02115

Abstract. *Drosophila melanogaster* (fruit fly) is a central organism in biology and is becoming increasingly important in the cardiovascular sciences. Prior work in optical imaging of the *D. melanogaster* heart has focused on static and dynamic structural anatomy. In the study, it is demonstrated that Doppler optical coherence tomography can quantify dynamic heart wall velocity and hemolymph flow in adult *D. melanogaster*. Since hemolymph is optically transparent, a novel exogenous contrast technique is demonstrated to increase the backscatter-based intracardiac Doppler flow signal. The results presented here open up new possibilities for functional cardiovascular phenotyping of normal and mutant *D. melanogaster*. [DOI: 10.1117/1.3503418]

Keywords: coherent optical systems; Doppler effect; flows; biomedical optics; biology.

Paper 09570R received Dec. 22, 2009; revised manuscript received Aug. 31, 2010; accepted for publication Aug. 31, 2010; published online Oct. 29, 2010.

1 Introduction

Over the past decade, there has been considerable growth in the literature focusing on the cardiovascular biology of *Drosophila melanogaster*. In particular, this research has focused on cardiovascular development[1] and on using *D. melanogaster* as a model for human cardiovascular disease.[2] Two main categories of innovations have driven this research. First, genetic and genomic technologies continue to increase in sophistication. Examples include the availability of deletion collections with high-resolution genomic coverage[3] and gene expression microarrays.[4] Second, there are a growing number of nonimaging and imaging technologies that allow for qualitative and quantitative assessment of *D. melanogaster* heart function. These techniques range from invasive point mea-

Address all correspondence to: Michael A. Choma, Yale University School of Medicine, Department of Diagnostic Radiology, MRRC, TAC N117, P.O. Box 208043, New Haven, Connecticut, 06520-8043. Tel: 203-785-2945; Fax: 203-785-6643; E-mail: michael.choma@yale.edu

1083-3668/2010/15(5)/056020/6/$25.00 © 2010 SPIE

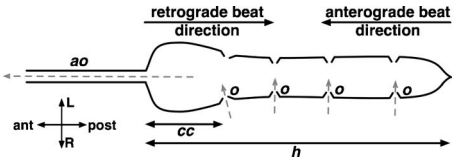

Fig. 1 Schematic of the heart (h) and proximal aorta (ao) in adult *D. melanogaster*.[30] Direction of hemolymph inflow through ostia (o) and outflow through the aorta (ao) is indicated by the dashed gray arrows. The heart is located in the abdomen, and the aorta originates near the junction of the abdomen and thorax. OCT imaging in this study focused on the conical chamber (cc), the most anterior portion of the heart. An anterograde beat is characterized by posterior-to-anterior contraction of the heart, while a retrograde beat is characterized by anterior-to-posterior contraction of the heart.

surements of heart electrical activity[5] to direct optical imaging of dynamic heart anatomy.[5–9]

Structural optical coherence tomography (OCT) has been previously employed to investigate the dynamic heart function of *D. melanogaster*.[6,7,10] This work builds on prior experience with OCT in vertebrate cardiovascular embryonic imaging.[11–19] In addition to focusing on static and dynamic heart anatomy, some of these vertebrate studies imaged blood flow using Doppler OCT.[12,15,18] The scattering-related Doppler signal exploited in these studies was generated by endogenous scatterers, i.e., red blood cells. *D. melanogaster*, however, relies on an extensive tracheal system for oxygen delivery[20,21] and, therefore, does not have red blood cells in its circulatory fluid or hemolymph. In fact, the adult hemolymph is relatively transparent when imaged using OCT.[6,7] Therefore, exogenous agents are required to perform Doppler-based flow imaging. Being able to perform flow imaging would be useful for detailed phenotyping of normal and mutant *D. melanogaster* cardiovascular physiology. In addition, flow imaging has the potential to study flow reversal (Fig. 1). Flow reversal is a normal occurrence in *D. melanogaster* and occurs when the heart switches from anterograde contractions to retrograde contractions or vice versa.[22] The specific physiological role of flow reversal in *D. melanogaster* is incompletely understood and, as such, is an active area of investigation.[23] In particular, it is unclear whether heartbeat reversal in *D. melanogaster* drives shifts in hemolymph volume between body segments to influence tracheal ventilation as it does in insects such as adult butterflies.[23] Prior research efforts into the mechanisms behind and physiologic role of flow reversal have focused on heart wall motion[22–24] and not directly on flow itself.

In addition to providing information regarding cardiovascular flow, Doppler-based imaging can provide information about heart wall motion. In clinical cardiology, heart wall velocimetry using ultrasound imaging[25] can be used obtain information about systolic and diastolic function.[26] Doppler wall velocimetry using OCT may therefore provide similar information in the imaging of small cardiovascular systems such as *D. melanogaster* and developing embryos. In this study, we demonstrate the feasibility of using Doppler OCT for quantitatively studying cardiac flow and wall motion in adult *D. melanogaster*. Two sets of results are presented here. First, B- and M-mode Doppler OCT were used to perform heart wall velocimetry in wild-type adult *D. melanogaster* hearts. Second, intracardiac Doppler OCT flow imaging was achieved by introducing scattering polystyrene microspheres into the open circulation using a novel microinjection technique.

2 Methods

2.1 *D. melanogaster Culture, Anesthesia, and Immobilization*

Flies (OreR) were raised at 24 °C and fed an instant food media (Carolina Biological Supply Company, Burlington, North Carolina). For contrast injection and imaging, flies were anesthetized with FlyNap (Carolina Biological Supply Company). FlyNap is a volatile mixture of triethylamine (50%), ethanol (25%), and fragrance (25%). After anesthesia, flies were immobilized by taping their wings to a glass slide.

2.2 *OCT System and Imaging*

OCT imaging focused on the conical chamber of the heart (Fig. 1). The principles and operation of the phase-sensitive OCT system used has been previously described.[27] Briefly, this optical frequency domain–type OCT system employed a swept laser source with a semiconductor optical amplifier gain medium and a scanning polygon-based wavelength filter. The system operates at a center wavelength of ~1300 nm and has an axial resolution of ~10 μm in air. Imaging was performed at A-line rates of 10 kHz. The sample arm optics have a predicted lateral resolution of 16 μm.

This OCT system tracks the phase-sensitive time-domain signal by calculating the change between successive A-scans in the phase of the fast Fourier transform of the wave number–domain spectral interferogram. As previously described,[27,28] swept laser sources with a mechanical wavelength-tuning element have an intrinsic source of phase instability in that each sweep of the laser has a slightly different starting wave number. In order to correct for this, the phase of an independent stationary sample mirror was recorded in order to establish a zero-phase point when calculating the phase difference on successive A-scans.[27] Doppler shifts (f_d) were converted to velocity (v) using the usual Doppler equation [$f_d = 2v\cos(\theta)n\nu/c$; θ, Doppler angle; n, tissue optical index; ν, optical frequency; c, free-space vacuum speed of light].

2.3 *Exogenous Contrast*

A novel microinjection technique was used to visualize intracardiac flow (Fig. 2(a); Video 1). Using a micropipette puller, glass capillary tubes (outer diameter 1 mm) were tapered and then cleaved on a rough surface to a final tip outer diameter of ~100 μm. Next, 830-nm red polystyrene beads (Bangs Laboratories, Fishers, Indiana) were diluted 3:1 with normal saline. The contrast solution was formulated immediately prior to injection. Particle uniformity was ensured by thoroughly mixing the solution by repeated intake into and ejection from a micropipette tip over the course of ~1 min. Injections were performed under a standard stereomicroscope. After manually introducing a contrast agent-filled micropipette into the thorax, contrast was injected by applying 3 psi of pressure applied over 30 ms using a nitrogen-based pressure injection system. Exogenous injection was performed us-

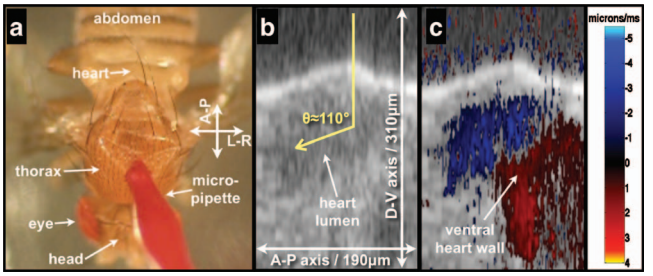

Fig. 2 Intraluminal Doppler OCT imaging using exogenous scattering contrast agents. Panel (a) is a still frame taken from Video 1 and shows the microinjection technique. Panel (b) is a structural OCT image of the heart during systole a few minutes after injection of contrast agent into the thorax. Panel (c) has the Doppler OCT image superimposed on the structural OCT image. The Doppler angle is estimated to be 110 deg. Also clearly seen in panel (c) is the Doppler signal generated by the ventral wall.

ing light stereomicroscopy guidance. OCT imaging was performed a few minutes after injection.

2.4 *Image Processing*

Images were acquired using custom-designed LabView (National Instruments, Austin, Texas) software. MATLAB (MathWorks, Natick, Massachusetts) and ImageJ[29] were used for advanced processing. Doppler signal from areas of low backscatter intensity (e.g., air, transparent fluid) was rejected based on pixel intensity in structural images.

3 Results

Figure 3 shows B-mode structural and Doppler OCT images as the heart completes one cycle of contraction (i.e., systole) and relaxation (i.e., diastole). An anterograde (i.e., posterior to anterior) beat[22] is shown. Prior to contraction, there was no organized Doppler signal from the heart wall. During systole, the Doppler signal on the ventral wall clearly traveled from the posterior to anterior aspect of the heart chamber. Futhermore, prior to discernable change in heart chamber diameter, a positive Doppler signal was detected from the posterior aspect of the ventral heart wall. Peak ventral wall velocity in Fig. 2 was ~1 μm/ms (~1 mm/s). It was assumed that wall motion was parallel to the direction of sample arm OCT beam propagation. Given a measured dorsal–ventral diastolic

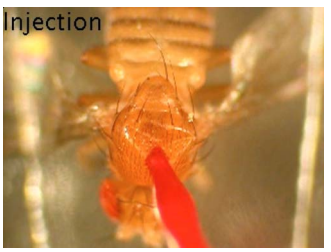

Video 1 Injection of exogeneous scattering contrast particles. The first 15 s of the video show microinjection of the particles into the thorax. The last 3 s focus on the heart of the same animal after injection. The heart can be readily identified by red particles that have adhered to its lumen. (Color online only.) (QuickTime, 3.26 MB) [URL: http://dx.doi.org/10.1117/1.3503418.1].

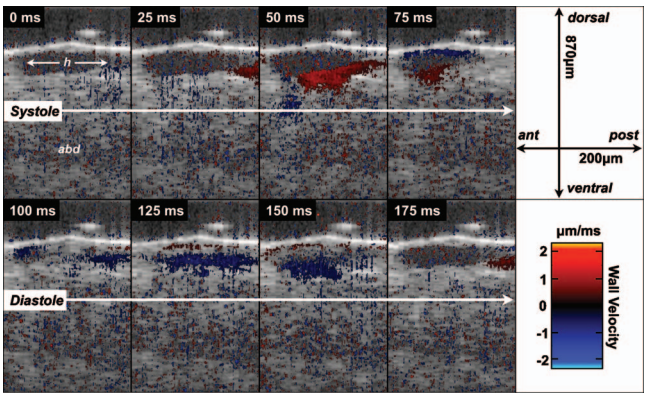

Fig. 3 High temporal resolution structural and Doppler OCT imaging (40 frames per second) of dynamic anatomy and heart wall velocity during an anterograde (posterior-to-anterior) heart beat in *D. melanogaster*. Also note that the lumen during systole generated very little backscatter-related signal, and as a consequence, there is essentially no flow-related Doppler signal.

diameter of ~100 μm in this individual fly, the wall velocity normalized to chamber diameter was ~10 chamber diameters per second. During systole, the Doppler signals from the ventral and dorsal walls had opposite signs, indicating that the heart wall was moving oppositely. During diastole, the direction of heart wall relaxation was also in a posterior-to-anterior direction. The magnitude of the ventral wall's Doppler signal during diastole was slightly less than the magnitude during systole.

Figure 4 shows an M-mode structural and Doppler OCT

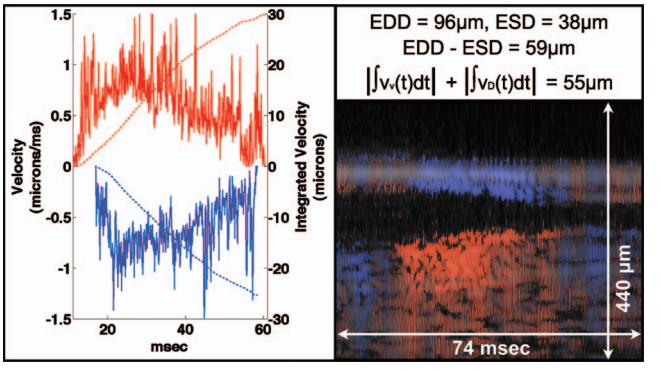

Fig. 4 Dorsal and ventral heart wall velocity (left panel) during systole as measured using M-mode Doppler OCT (lower-right panel). These representative velocity curves were obtained by plotting the maximum (ventral wall) or minimum (dorsal wall) wall velocity at each time point (i.e., M-mode line) from a manual region of interest drawn on each heart wall. Red curves are ventral data, and blue curves are dorsal data. Solid curves represent velocity data, while dashed curves represent displacement (i.e., integrated velocity) data. The upper-right panel shows the equations governing change in chamber diameter measured using structural OCT and calculation of displacement using Doppler velocimetry data. The structural OCT image is shadowed over the Doppler M-mode image. The red/blue (i.e., positive/negative Doppler shift) color map used here is distinct from that used in the other figures and has a very limited dynamic range in order to accentuate the sign, as opposed to the magnitude, of the Doppler shift. EDD, end-diastolic diameter; ESD, end-systolic diameter; $v_v(t)$, time-varying ventral wall velocity; $v_D(t)$, time-varying dorsal wall velocity.

Video 2 Thoracic injection of an absorptive red dye. Immediately after injection, a "blush" of dye can be seen in the heart. (QuickTime, 670 KB) [URL: http://dx.doi.org/10.1117/1.3503418.2].

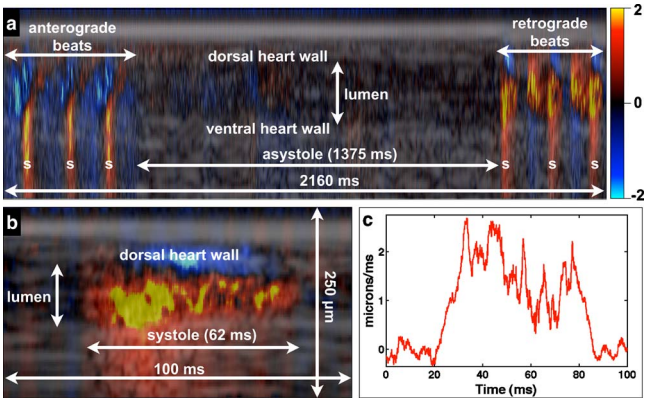

Fig. 5 Intracardiac M-mode Doppler flow imaging several minutes after the injection of exogenous contrast material. Panel (a) shows an extended M-mode recording that captures cardiac reversal. Flow related to anterograde beats generated a negative Doppler shift, while flow related to retrograde beats generated a positive Doppler shift. Systole (s) was determined by the presence of a positive Doppler shift on the ventral heart wall. Panel (b) shows the first retrograde systolic event after asystole, while panel (c) shows the midline velocity profile from (b). Both (a) and (b) have a height of 250 μm.

image of the heart during systole. By using M-mode imaging at an A-scan rate of 10 kHz, measurement of wall velocity was obtained in the millisecond regime. The time-varying ventral and dorsal heart wall velocities during systole are plotted. The ventral wall velocity magnitude was slightly larger than that of the dorsal wall velocity. The integrated velocities for each wall corresponded to the total measured change in dorsal–ventral chamber diameter. The total measured change corresponds to the difference between the manually measured end-diastolic diameter (EDD) and the end-systolic diameter (ESD) of the heart lumen along the dorsal–ventral axis.

As discussed earlier and as evident from Figs. 3 and 4, adult *D. melanogaster* hemolymph is essentially transparent. Its transparency is related to its low fractional particle volume (i.e., percent volume of a fluid mixture that is a cell or another kind of particle). The fractional particle volume can in principle be increased by introduction of microparticles into the circulatory flow. Since hemolymph in the extracellular–extravascular space (e.g., hemocoel) flows into the heart via ostia (Fig. 1), any particle injected into the extracellular–extravascular space should flow into the heart, provided that the particle is smaller than the ostia diameter. Since ostia in the adult *D. melanogaster* have a diameter of $\sim$10 μm (Ref. 30), microparticles should readily pass into the heart. This was confirmed experimentally (Fig. 2; Video 1). Video 1 is a 15-fps video recording of microparticle microinjection. After introduction of the micropipette into the thorax and injection of the particles, a "blush" of red was seen at the presumed location of the heart just posterior to the thorax–abdomen junction. The distribution and flow of particles appeared directed and not isotropic. After several seconds, the blush cleared. Zooming in on the heart, there was a faint red outline of the heart due to microparticles sticking presumably to the lumen of the heart. As a secondary confirmation of this mode of contrast delivery in the adult *D. melanogaster* cardiovascular system, red dye (McCormick and Company, Sparks, Maryland) injected into the thorax localized to the heart as observed on video microscopy (Video 2).

Structural OCT imaging, performed a few minutes after injection, showed significant intracardiac backscatter signal (Fig. 2), demonstrating that OCT can detect backscatter from a steady-state concentration of microparticles, long after the color of the microparticle is no longer visible in the hemolymph by light microscopy. This backscatter signal enabled intraluminal flow imaging using Doppler OCT. The presence of Doppler signal of significant magnitude corresponded with the onset of wall motion as indicated by wall Doppler signal. The flow-related Doppler signal during systole had a negative sign, indicating an anterograde (i.e., posterior-to-anterior) flow. For comparison, note the relative absence of OCT Doppler signal in the heart lumen in the absence of exogenous contrast (Figs. 3 and 4). Overall, seven OCT-confirmed and one video microscopy–confirmed injections of microparticles were successfully completed.

Figure 5 shows an extended M-mode recording that demonstrates the phenomenon of cardiac reversal.[22] During cardiac reversal, the direction of the heart contractions reverse. Over the course of the 2.16-s M-mode image in Fig. 5(a), the heart transitioned from anterograde contraction to asystole to retrograde (i.e., anterior-to-posterior) contractions. As in Fig. 2, flow generated by anterograde contractions generated a Doppler shift with a negative sign. During asystole, there was no significant intraluminal or heat wall Doppler signal. During retrograde contractions, the flow-generated Doppler shift had a positive sign, indicating anterior-to-posterior flow. These results indicate that flow direction can be determined with a one-dimensional spatial flow measurement, whereas heart wall Doppler imaging requires a two-dimensional Doppler measurement (Fig. 3). Figure 5(b) shows the first systolic event after the $\sim$1.375-s asystolic period, while Fig. 5(c) is a plot of the midline intraluminal flow velocity taken over a narrow rectangular region of interest, with each time point representing an average over the spatial dimension of the region of interest. Rapid flow acceleration on the order of 0.1 μm/ms^2 ($\sim$2 μm/ms/20 ms) could be estimated from the flow profile.

Formal survival studies after microinjection were not performed. However, in our initial experience with eight flies with imaging-confirmed injection of a scattering contrast agent, flies would live for a few to several hours after injection of the polystyrene microspheres.

4 Discussion

The proof-of-principle results shown here represent the first use of Doppler OCT to quantify cardiovascular function in the adult *D. melanogaster*. Heart wall velocimetry is readily accomplished in the millisecond regime. This is important because the time constant of cardiovascular mechanics are on the order of milliseconds. The open circulatory physiology of this animal is exploited to deliver, in a straightforward manner, scattering contrast agents into the heart, thereby enabling Doppler OCT flow imaging. Moreover, during an anterograde beat, ventral heart wall and intraluminal Doppler signal are readily distinguished from each other.

Doppler OCT thus has the potential to enhance the use of adult *D. melanogaster* as a model of cardiovascular disease. Prior imaging studies have relied on phenotypes (e.g., heart rate, fractional shortening) derived from direct observation and from dynamic structural heart parameters (e.g., end-diastolic and end-systolic diameters).[5,6,9,10] Through phase-sensitive detection and processing, the repertoire of cardiovascular phenotypes for genetic screens can be expanded to include heart wall velocity and intracardiac flow velocity. Future work on contrast imaging will address three limitations in the present study. First, anesthesia may have direct cardiac effects, and our work has shifted to the prepupal stage when the organism is immobile and anesthesia is not required for cardiac imaging. Second, the increased fractional particle volume of contrast-enhanced hemolymph can increase the hemolymph viscosity. Therefore, future work will focus on minimizing the injected volume of contrast agent while maintaining sufficient backscatter signal for Doppler imaging. Third, intraluminal and heart wall Doppler signal can be difficult to distinguish when they are of the same sign. Differentiation between the two could potentially be made based on the standard deviation of the Doppler signal.[31]

In this and prior[7] studies, the heart wall speckle pattern is relatively static when the heart is at rest but varies rapidly during contraction and relaxation. Such variations in speckle influences the signal-to-noise ratio of the heart wall Doppler signal.[32] Although spatial and temporal averaging can improve the signal-to-noise ratio in this context, such prominent variations in speckle can be potentially utilized for heart wall elastography using previously described methods (see, for example, Ref. 33).

In addition to its importance in the study of heart development and human cardiovascular disease, *D. melanogaster* is of biologic interest because it has an open circulation. Open circulations are of evolutionary and physiologic interest. Given that open circulatory dynamics are not as well defined as those of closed circulation, and given a growing appreciation and understanding of the complexity and diversity of open circulations (see, for example, Ref. 23), Doppler OCT in *D. melanogaster* may have broad interest in biology.

Acknowledgments

This work was generously supported by the Frederick H. Lovejoy Fund, Children's Hospital Boston (MAC) and by an American Medical Association Foundation Seed Grant (MAC). We additionally acknowledge funding support from NIH R01HL076398 and NIH R01CA103769 (development of the imaging system) and from the Department of Defense Air Force Office of Scientific Research, Medical Free Electron Laser Program FA9550-04-1-0079.

References

1. Y. Tao and R. A. Schulz, "Heart development in *Drosophila*," *Semin Cell Dev. Biol.* **18**(1), 3–15 (2007).
2. E. Bier and R. Bodmer, "*Drosophila*, an emerging model for cardiac disease," *Gene* **342**(1), 1–11 (2004).
3. A. L. Parks, K. R. Cook, M. Belvin, N. A. Dompe, R. Fawcett, K. Huppert, L. R. Tan, C. G. Winter, K. P. Bogart, J. E. Deal, M. E. Deal-Herr, D. Grant, M. Marcinko, W. Y. Miyazaki, S. Robertson, K. J. Shaw, M. Tabios, V. Vysotskaia, L. Zhao, R. S. Andrade, K. A. Edgar, E. Howie, K. Killpack, B. Milash, A. Norton, D. Thao, K. Whittaker, M. A. Winner, L. Friedman, J. Margolis, M. A. Singer, C. Kopczynski, D. Curtis, T. C. Kaufman, G. D. Plowman, G. Duyk, and H. L. Francis-Lang, "Systematic generation of high-resolution deletion coverage of the *Drosophila melanogaster* genome," *Nat. Genet.* **36**(3), 288–292 (2004).
4. B. Zeitouni, S. Senatore, D. Severac, C. Aknin, M. Semeriva, and L. Perrin, "Signalling pathways involved in adult heart formation revealed by gene expression profiling in *Drosophila*," *PLoS Genet* **3**(10), 1907–1921 (2007).
5. K. Ocorr, N. L. Reeves, R. J. Wessells, M. Fink, H. S. Chen, T. Akasaka, S. Yasuda, J. M. Metzger, W. Giles, J. W. Posakony, and R. Bodmer, "KCNQ potassium channel mutations cause cardiac arrhythmias in *Drosophila* that mimic the effects of aging," *Proc. Natl. Acad. Sci. U.S.A.* **104**(10), 3943–3948 (2007).
6. M. J. Wolf, H. Amrein, J. A. Izatt, M. A. Choma, M. C. Reedy, and H. A. Rockman, "*Drosophila* as a model for the identification of genes causing adult human heart disease," *Proc. Natl. Acad. Sci. U.S.A.* **103**(5), 1394–1399 (2006).
7. M. A. Choma, S. D. Izatt, R. J. Wessells, R. Bodmer, and J. A. Izatt, "*In vivo* imaging of the adult *Drosophila melanogaster* heart with real-time optical coherence tomography," *Circulation* **114**(2), E35–E36 (2006).
8. B. Monier, M. Astier, M. Semeriva, and L. Perrin, "Steroid-dependent modification of Hox function drives myocyte reprogramming in the *Drosophila* heart," *Development* **132**(23), 5283–5293 (2005).
9. K. A. Ocorr, T. Crawley, G. Gibson, and R. Bodmer, "Genetic variation for cardiac dysfunction in *Drosophila*," *PLoS ONE* **2**(7), e601 (2007).
10. M. J. Allikian, G. Bhabha, P. Dospoy, A. Heydemann, P. Ryder, J. U. Earley, M. J. Wolf, H. A. Rockman, and E. M. McNally, "Reduced life span with heart and muscle dysfunction in *Drosophila sarcoglycan* mutants," *Hum. Mol. Genet.* **16**(23), 2933–2943 (2007).
11. S. A. Boppart, G. J. Tearney, B. E. Bouma, J. F. Southern, M. E. Brezinski, and J. G. Fujimoto, "Noninvasive assessment of the developing *Xenopus* cardiovascular system using optical coherence tomography," *Proc. Natl. Acad. Sci. U.S.A.* **94**(9), 4256–4261 (1997).
12. S. Yazdanfar, M. D. Kulkarni, and J. A. Izatt, "High-resolution imaging of *in vivo* cardiac dynamics using color Doppler optical coherence tomography," *Opt. Express* **1**(13), 424–431 (1997).
13. T. M. Yelbuz, M. A. Choma, L. Thrane, M. L. Kirby, and J. A. Izatt, "Optical coherence tomography—a new high-resolution imaging technology to study cardiac development in chick embryos," *Circulation* **106**(22), 2771–2774 (2002).
14. M. W. Jenkins, D. C. Adler, M. Gargesha, R. Huber, F. Rothenberg, J. Belding, M. Watanabe, D. L. Wilson, J. G. Fujimoto, and A. M. Rollins, "Ultrahigh-speed optical coherence tomography imaging and visualization of the embryonic avian heart using a buffered Fourier domain mode locked laser," *Opt. Express* **15**(10), 6251–6267 (2007).
15. A. Mariampillai, B. A. Standish, N. R. Munce, C. Randall, G. Liu, J. Y. Jiang, A. E. Cable, I. A. Vitkin, and V. X. D. Yang, "Doppler optical cardiogram gated 2D color flow imaging at 1000 fps and 4D *in vivo* visualization of embryonic heart at 45 fps on a swept source OCT system," *Opt. Express* **15**(4), 1627–1638 (2007).
16. M. W. Jenkins, F. Rothenberg, D. Roy, V. P. Nikolski, Z. Hu, M. Watanabe, D. L. Wilson, I. R. Efimov, and A. M. Rollins, "4D embryonic cardiography using gated optical coherence tomography," *Opt. Express* **14**(2), 736–748 (2006).

17. M. W. Jenkins, P. Patel, H. Y. Deng, M. M. Montano, M. Watanabe, and A. M. Rollins, "Phenotyping transgenic embryonic murine hearts using optical coherence tomography," *Appl. Opt.* **46**(10), 1776–1781 (2007).
18. A. M. Davis, F. G. Rothenberg, N. Shepherd, and J. A. Izatt, "*In vivo* spectral domain optical coherence tomography volumetric imaging and spectral Doppler velocimetry of early stage embryonic chicken heart development," *J. Opt. Soc. Am. A* **25**(12), 3134–3143 (2008).
19. R. Yelin, D. Yelin, W.-Y. Oh, S. H. Yun, C. Boudoux, B. J. Vakoc, B. E. Bouma, and G. J. Tearney, "Multimodality optical imaging of embryonic heart microstructure," *J. Biomed. Opt.* **12**(6), 064021 (2007).
20. J. H. Law and M. A. Wells, "Insects as biochemical models," *J. Biol. Chem.* **264**(28), 16335–16338 (1989).
21. T. Burmester and T. Hankeln, "The respiratory proteins of insects," *J. Insect Physiol.* **53**(4), 285–294 (2007).
22. D. Dulcis and R. B. Levine, "Innervation of the heart of the adult fruit fly, *Drosophila melanogaster*," *J. Comp. Neurol.* **465**(4), 560–578 (2003).
23. L. T. Wasserthal, "*Drosophila* flies combine periodic heartbeat reversal with a circulation in the anterior body mediated by a newly discovered anterior pair of ostial valves and 'venous' channels," *J. Exp. Biol.* **210**(Pt 21), 3707–3719 (2007).
24. D. Dulcis and R. B. Levine, "Glutamatergic innervation of the heart initiates retrograde contractions in adult *Drosophila melanogaster*," *J. Neurosci.* **25**(2), 271–280 (2005).
25. K. Isaaz, A. Thompson, G. Ethevenot, J. L. Cloez, B. Brembilla, and C. Pernot, "Doppler echocardiographic measurement of low-velocity motion of the left ventricular posterior wall," *Am. J. Cardiol.* **64**(1), 66–75 (1989).
26. N. R. Van de Veire, J. De Sutter, J. J. Bax, and J. R. Roelandt, "Technological advances in tissue Doppler imaging echocardiography," *Heart (Br. Cardiac Soc.)* **94**(8), 1065–1074 (2008).
27. B. J. Vakoc, S. H. Yun, J. F. de Boer, G. J. Tearney, and B. E. Bouma, "Phase-resolved optical frequency domain imaging," *Opt. Express* **13**(14), 5483–5493 (2005).
28. M. A. Choma, A. K. Ellerbee, C. Yang, T. L. Creazzo, and J. A. Izatt, "Spectral-domain phase microscopy," *Opt. Lett.* **30**(10), 1162–1164 (2005).
29. W. S. Rasband, *ImageJ*, National Institutes of Health, Bethesda, MD (1997–2009).
30. N. J. Curtis, J. M. Ringo, and H. B. Dowse, "Morphology of the pupal heart, adult heart, and associated tissues in the fruit fly, *Drosophila melanogaster*," *J. Morphol.* **240**(3), 225–235 (1999).
31. Y. H. Zhao, Z. P. Chen, C. Saxer, Q. M. Shen, S. H. Xiang, J. F. de Boer, and J. S. Nelson, "Doppler standard deviation imaging for clinical monitoring of *in vivo* human skin blood flow," *Opt. Lett.* **25**(18), 1358–1360 (2000).
32. M. A. Choma, A. K. Ellerbee, S. Yazdanfar, and J. A. Izatt, "Doppler flow imaging of cytoplasmic streaming using spectral domain phase microscopy," *J. Biomed. Opt.* **11**(2), 024014 (2006).
33. J. M. Schmitt, "OCT elastography: imaging microscopic deformation and strain of tissue," *Opt. Express* **3**(6), 199–211 (1998).